polymer

The sub-T_g relaxations in pure and antiplasticized model epoxy networks as studied by high resolution creep rate spectroscopy

V.A. Bershtein[a], N.N. Peschanskaya[a], J.L. Halary[b,*], L. Monnerie[b]

[a]*Ioffe Physico-Technical Institute of the Russian Academy of Sciences, 194021 St. Petersburg, Russia*
[b]*Laboratoire de Physicochimie Structurale et Macromoléculaire (UMR 7615), Ecole Supérieure de Physique et Chimie Industrielles de la Ville de Paris, 75231 Paris, Cedex 05, France*

Abstract

An original laser-interferometric creep rate spectroscopy method was used for studying the molecular mobility in the glassy state of a series of 'model' epoxy-amine networks varying in cross-link density and rigidity. The experiments were carried out over the temperature range 115–300 K, which covers the regions where the secondary relaxations are expected to occur. The creep rate spectra (CRS) obtained at low compressive stresses exhibited systematically multiple creep rate $\dot{\varepsilon}$ peaks, irrespective of the applied stress and the experimental time in the ranges under consideration, namely 20–40 MPa and 10–40 s, respectively. Data analysis was based on the inspection of the major peaks of the CRS without entering much into the details of the fine structure. The peaks assigned to the β relaxation were shown to depend on the changes in network cross-link density and to the addition of antiplasticizing molecules in the same way as reported earlier from dynamic mechanical analysis (DMA) and ^{13}C nuclear magnetic resonance (NMR) studies. In the case of the resins cured with aromatic amines, for which no γ relaxation is evidenced by DMA, creep rate spectroscopy allowed the detection of an additional relaxation, so called γ', at temperatures well below the β process. It was tentatively assigned to DMA-inactive motions of the aromatic amine residues, i.e. to the phenyl ring flips of the diphenylmethane units. © 1999 Elsevier Science Ltd. All rights reserved.

Keywords: Epoxy networks; Creep rate spectroscopy; Sub-T_g relaxations

1. Introduction

During the past decades, the epoxy resins have been the subject of numerous studies. Among them, particular attention [1–8] has been paid to the epoxy-amine networks based on diglycidylether of bisphenol A (DGEBA) and 4,4'-diaminodiphenylmethane (DDM) or hexamethylenediamine (HMDA). The use of these two curing agents led to networks presenting similar cross-link densities but to substantial differences in chain rigidity and, as a consequence, in glass transition temperature T_g. In addition, mixtures of these primary diamines with their homologous primary monoamines or secondary diamines were used to allow the cross-link density of the networks to vary without significant modifications in their chemical structure. Now, such materials whose architecture, kinetics of formation [3,4], dynamic mechanical properties [1,2,6], and chain packing characteristics [7] has been extensively discussed can be regarded as 'model' networks.
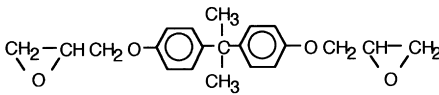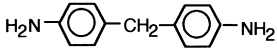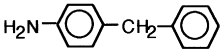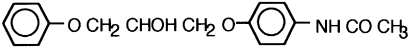
One of the typical features of these epoxy networks is the occurrence of strong sub-T_g relaxations. On the dynamic mechanical traces, the secondary β process shows up over a broad temperature range (typically 120–300 K, respectively in the case of the DGEBA–DDM and DGEBA–HMDA networks studied at a frequency of $\nu = 1$ Hz). It has been shown [2,6] that the extent of this relaxation depends strongly on the architecture of the network: the lower the cross-link density, the narrower the temperature range covered and the weaker the mechanical damping. Antiplasticization of the fully cross-linked networks was shown to provoke the same effects on the β relaxation peak as the reduction of the cross-link density [9]. In addition, another mechanically active secondary relaxation, so-called γ, has been observed at lower temperatures in the case of networks presenting sufficiently long aliphatic sequences [10,11], either in the epoxide moiety or in the amine unit. As an example, the γ process was detected on the dynamic mechanical traces relative to the DGEBA networks of the HMDA series, but not on the traces relative to the DGEBA–DDM series [2].

The high-resolution solid state nuclear magnetic resonance (NMR) has proven to be a powerful tool for the

* Corresponding author. Tel.: + 33-1-40-79-46-79; fax: + 33-1-40-79-46-86.

E-mail address: Jean-Louis.Halary@espci.fr (J.L. Halary)

Table 1
Chemical formulae and origin of the chemicals used for the preparation of the epoxy networks

Chemical	Formula	Origin
DGEBA	$CH_2\text{--}CHCH_2\text{--}O\text{--}C_6H_4\text{--}C(CH_3)_2\text{--}C_6H_4\text{--}O\text{--}CH_2CH\text{--}CH_2$ (with epoxide O)	Bakelite (Rutapox 162)
4,4' diaminodiphenyl methane	$H_2N\text{--}C_6H_4\text{--}CH_2\text{--}C_6H_4\text{--}NH_2$	Fluka
4-benzyl aniline	$H_2N\text{--}C_6H_4\text{--}CH_2\text{--}C_6H_5$	Our laboratory [22,23]
HMDA	$H_2N\text{--}(CH_2)_6\text{--}NH_2$	Aldrich
Hexylamine (HA)	$H_2N\text{--}(CH_2)_5\text{--}CH_3$	Merck
Antiplasticizer (AP)	$C_6H_5\text{--}O\,CH_2\,CHOH\,CH_2\,O\text{--}C_6H_4\text{--}NH\,CO\,CH_3$	Our laboratory (as described in Ref. [9])

assignment of the sub-T_g transitions [5,6,9,12,13]. The γ relaxation observed in the DGEBA–HMDA series was unambiguously related to motions of the central CH$_2$'s of the hexamethylene sequences. The origin of the β relaxation was shown to be much more complex for two main reasons. Firstly, it is likely that two types of units are involved in the molecular motions which develop over the temperature range where the β transition is observed by the NMR methods, namely the motions of the hydroxypropylether –CH$_2$–CHOH–CH$_2$–O– moieties and the DGEBA ring flips [6,12,13]. Secondly, the spatial scale of the motions depends on both temperature and network architecture. Localized motions at the scale of an epoxy-amine repeat unit, were shown to occur at low temperature irrespective of the network. However, cooperative modes implying several repeat units would be responsible for the additional damping, which is observed on the high temperature side of the relaxation when the cross-link density is increased, and which exhibits a certain deviation from non-cooperative Arrhenius behavior. This interpretation is consistent with the results relative to the antiplasticized fully cross-linked networks [9,14]: the antiplasticizer, however, was shown to impede the mobility of the cross-link points and therefore to prevent (or reduce) the occurrence of cooperative motions.

Regarding the complexity of the sub-T_g β relaxation in epoxy networks, it was desirable to get further information on these phenomena by using additional experimental techniques. Among the possible ones, creep rate spectroscopy has proven for a long time to be a very powerful tool for the study of deformation kinetics at high stresses [15–17] and for the characterization of molecular motions in solids, by using small stresses, especially in polymers and multicomponent polymeric systems [15,18–21].

The goal of the present study is to take advantage of the high resolution of the laser-interferometric creep rate spectroscopy to support the main features of the sub-T_g relaxations of epoxy networks. To this end, selected systems were chosen in this publication by accounting for the effects of cross-link density, chain rigidity and antiplasticization.

2. Experimental

2.1. Materials

The characteristics of the chemicals used for the preparation of the networks are given in Table 1. The grade of epoxide used in this study (RUTAPOX 0162 from Bakelite) is of high purity and roughly free from polymerized epoxy units. Six networks were synthesized, namely: the fully cross-linked network DGEBA–DDM; three loosely cross-linked networks DGEBA–DDM/xBAN (where x is a figure representing the percentage of N–H reactive functions coming from the monoamine); the very loosely cross-linked and flexible network DGEBA–HMDA/95HA; and the antiplasticized fully cross-linked network DGEBA–DDM/0.62AP (where 0.62 represents the number of antiplasticizer molecules per hydroxypropylether moiety, calculated on the basis of a complete epoxide-amine reaction). The compositions of the initial mixtures are summarized in Table 2. It is worth noticing that the epoxide and amine N–H functions were maintained in stoichiometric proportions in all these mixtures. The chemical structure of the networks under consideration is schematically recalled in Fig. 1.

The networks were prepared according to the procedures detailed in our earlier publications for the pure [1,2,6] and for the antiplasticized [9,22] samples. The post-cure

Table 2
Code names, compositions and theoretical cross-link densities of the samples

Code name	mol% of diepoxide	mol% of diamine	mol% of third component	ξ (mol kg^{-1})
DGEBA–DDM	66.7	33.3	0	2.28
DGEBA–DDM/60BAN	55.6	11.1	33.3	0.82
DGEBA–DDM/80BAN	52.6	5.3	42.1	0.39
DGEBA–DDM/95BAN	50.6	1.3	48.1	0.10
DGEBA–HMDA/95HA	50.6	1.3	48.1	0.10
DGEBA–DDM/0.62AP	36.5	18.2	45.3	

at $T_g + 30$ K was performed to yield an epoxy-amine reaction as complete as possible. Under these conditions, no side reaction was observed and the number of unreacted functions is rather low [4]. The 'theoretical' cross-link densities, ξ, calculated by assuming complete reactions as a first approximation [22], are also given in the last entry of Table 2.

2.2. Creep rate spectroscopy

Fig. 2 schematizes the setup used for creep rate measure-

ments under uniaxial compression. It is based on a Michelson interferometer illuminated by a He–Ne laser (1). The optical part consists of three opaque mirrors (2–4) and two semi-transparent (half-silvered) ones (5 and 6). The mirror (2) is rigidly connected with the moving puncheon (11) following the deformation of the sample (12). The latter is loaded via the figured lever (15) for maintaining a constant stress whatever be the deformation conditions.

The laser beam is divided at the mirror (6) for two beams. The first one is reflected from the moving mirror (2) with a change in frequency resulting from the Doppler effect. The

Fig. 1. Schematic representation of the different types of networks: (a) fully cross-linked network DGEBA–DDM; (b) loosely cross-linked network DGEBA–DDM/BAN; (c) loosely cross-linked network DGEBA–HMDA/HA.
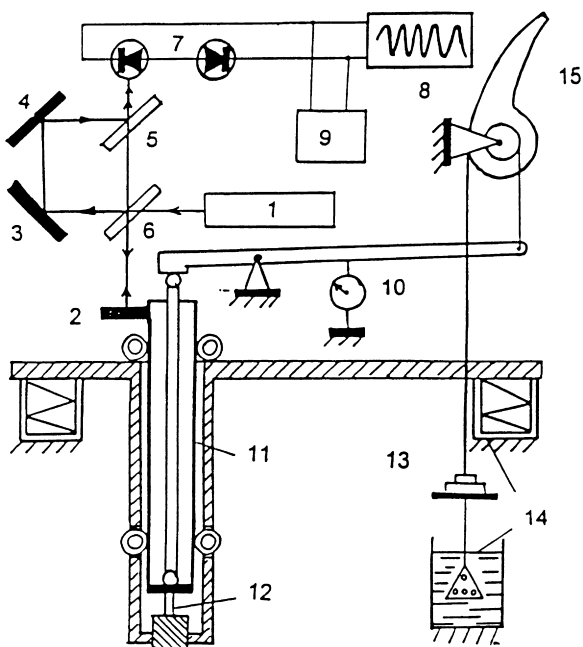
Fig. 2. Scheme of the interferometric setup for creep rate measurements under uniaxial compression: (1) laser; (2–4) opaque mirrors; (5,6) semi-transparent mirrors; (7) photocells; (8) recorder; (9) automatic section; (10) displacement gauge; (11) mobile puncheon; (12) sample; (13) load; (14) dampers; (15) figured lever providing a constant stress on the sample.

second beam is reflected from the opaque mirrors (3) and (4), and interferes at the mirror (5) with the beam of changed frequency. As a result, low-frequency beats arise in the resultant light beam. They are then transformed by the
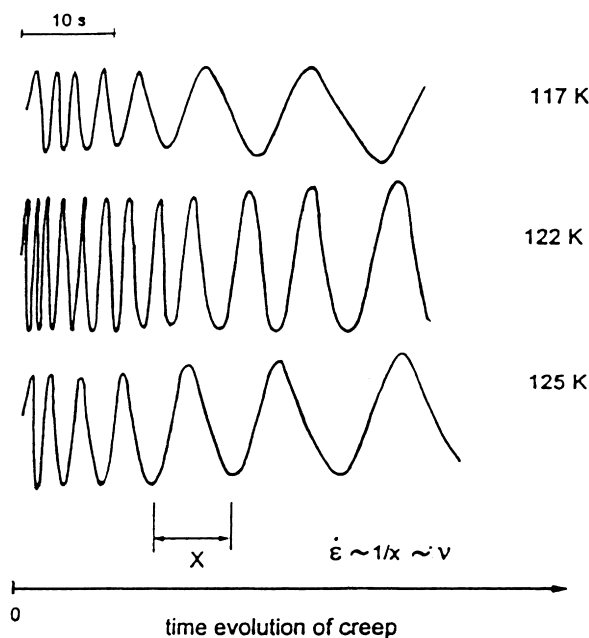
Fig. 3. Examples of typical creep rate interferograms. (network DGEBA–DDM/60BAN at the temperatures of the beginning, maximum and end of the creep rate peak; $\sigma = 20$ MPa; $t = 10$ s).

photocells (7) into an electric signal of identical frequency which is finally measured using standard instruments.

The time-dependent deformation is recorded in the form of a sequence of beats in an interferogram. Some examples of typical interferograms obtained in this way are shown in Fig. 3. The beat frequency, ν, and the number of oscillations, N, yield the creep rate $\dot{\varepsilon}$ and the deformation ε, respectively, from the following relations:

$$\varepsilon = \frac{\lambda \nu}{2I_0} \tag{1}$$

and

$$\varepsilon = \frac{\lambda N}{2I_0}, \tag{2}$$

where $\lambda = 630$ nm is the laser wavelength and I_0 is the initial length of the sample.

The creep rate spectra (CRS), showing the influence of temperature on $\dot{\varepsilon}$ values, were determined by using a unique sample over the broad temperature range under consideration (115–300 K). The cylindrical sample, 10 mm in height and 3 mm in diameter, was cooled down to the lowest temperature under study, and then subjected to a stress σ of usually 20 MPa and, occasionally, 40 MPa. Such applied stresses are much lower than the yield stress, but sufficiently high so that the sample can deform by about 0.01, and is solicitated in the non-linear (inelastic) domain of the stress–strain curve. Under these conditions, creep which develops was examined during 1 min by recording the relevant interferogram. After this first series of measurements, the sample was unloaded and heated up at a rate of 1 K min^{-1} until the next set of temperature measurements, which was 5–7 K higher than the previous one. The sample was then re-loaded to the same stress and the interferogram was recorded, and so on. Under the indicated conditions, creep is determined by the local shear strains, and its rate decreases as the process proceeds (see the interferograms in Fig. 3). Therefore, the creep rates are to be estimated at a given time t after the application of load. Depending on the experiments, three values of t were considered, namely 10, 30 and 40 s.

As a result of the high sensitivity of this technique, it was possible to determine the $\dot{\varepsilon}$ values by considering just one beat of the creep interferogram, i.e. a deformation increment as small as 300 nm. The accuracy of the $\dot{\varepsilon}$ determinations may be quoted to be about 1%, for creep rates in the range 10^{-6}–10^{-5} s^{-1}.

It is worth noting that the ultra-small changes in creep deformation which accompany the creep rate spectroscopy technique ensure that the isostructural state of the samples is to be maintained all over the measurements. This fact was corroborated by the systematic observation of the recovery of the initial creep rate after a back jump in temperature.
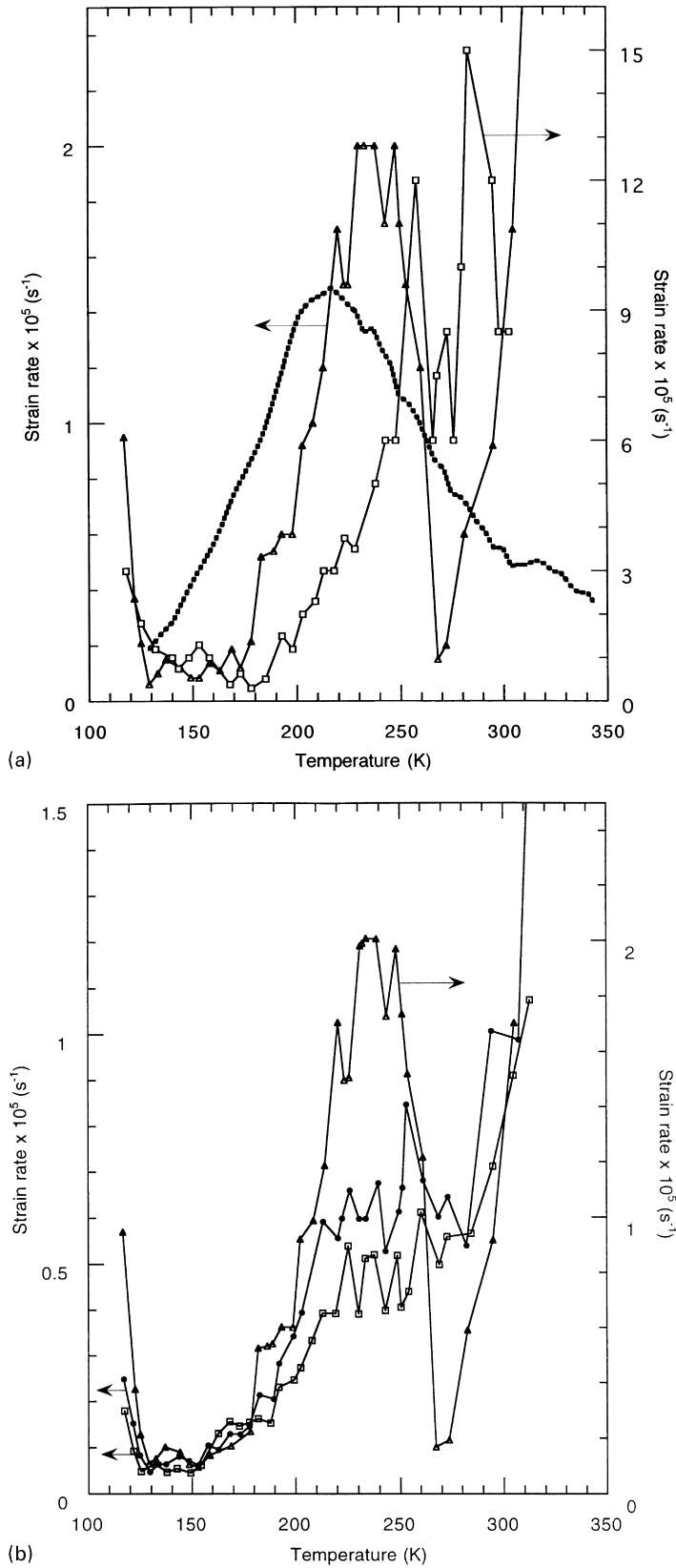
Fig. 4. CRS obtained for the DGEBA–DDM network: (a) at $t = 10$ s and $\sigma = 20$ MPa (triangles) or 40 MPa (squares). The dotted line corresponds to the E'' dynamic mechanical spectrum at 1 Hz (data taken from Ref. [23]) (b) at $\sigma = 20$ MPa and $t = 10$ s (triangles), 30 s (circles) or 40 s (squares).
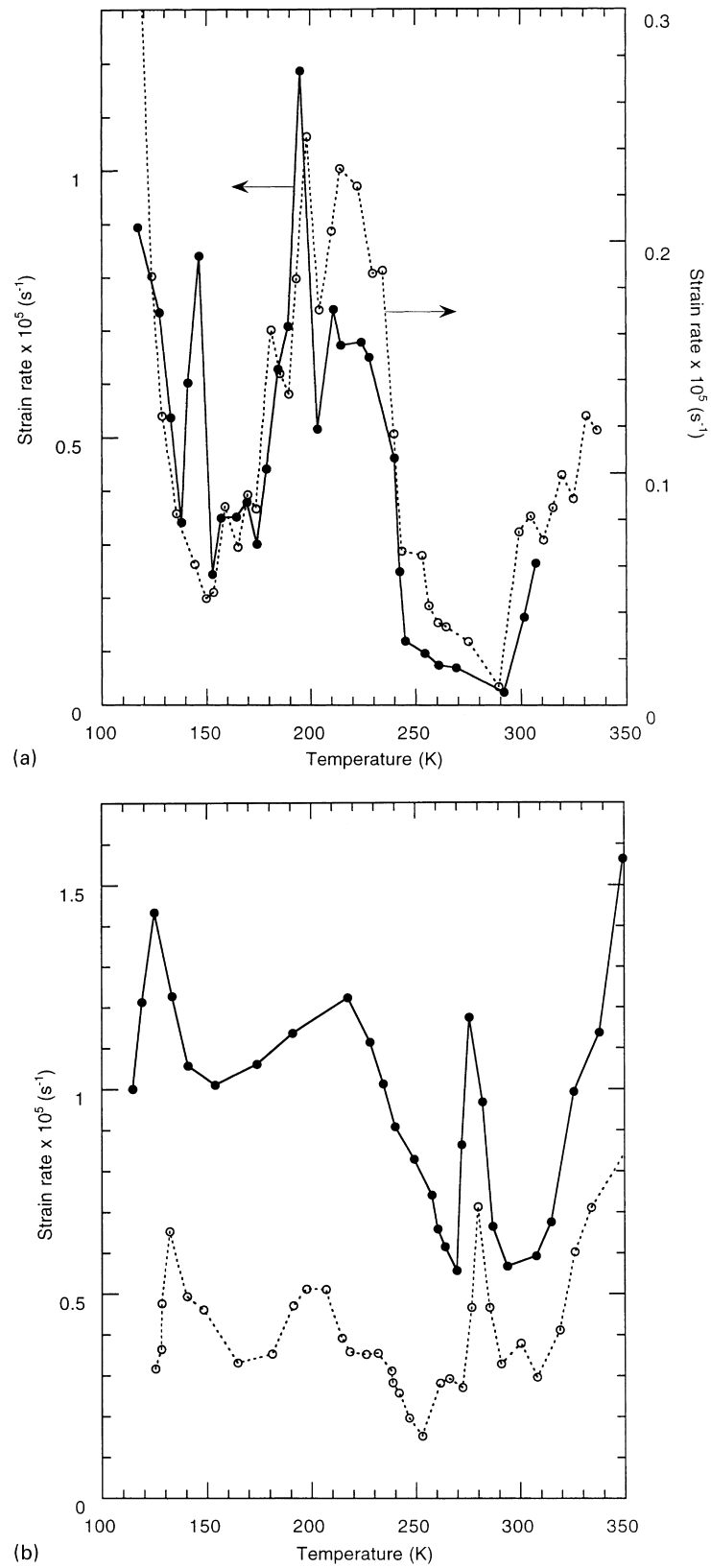
(a)

(b)

Fig. 5. CRS obtained at $\sigma = 20$ MPa for: (a) the DGEBA–DDM/80BAN network at $t = 10$ s (filled circles) or $t = 30$ s (open circles) (b) the DGEBA–DDM/95BAN system at $t = 10$ s (filled circles) or $t = 30$ s (open circles) (c) the DGEBA–HMDA/95HA system at $t = 10$ s (filled circles) or $t = 30$ s (open circles).

(c)
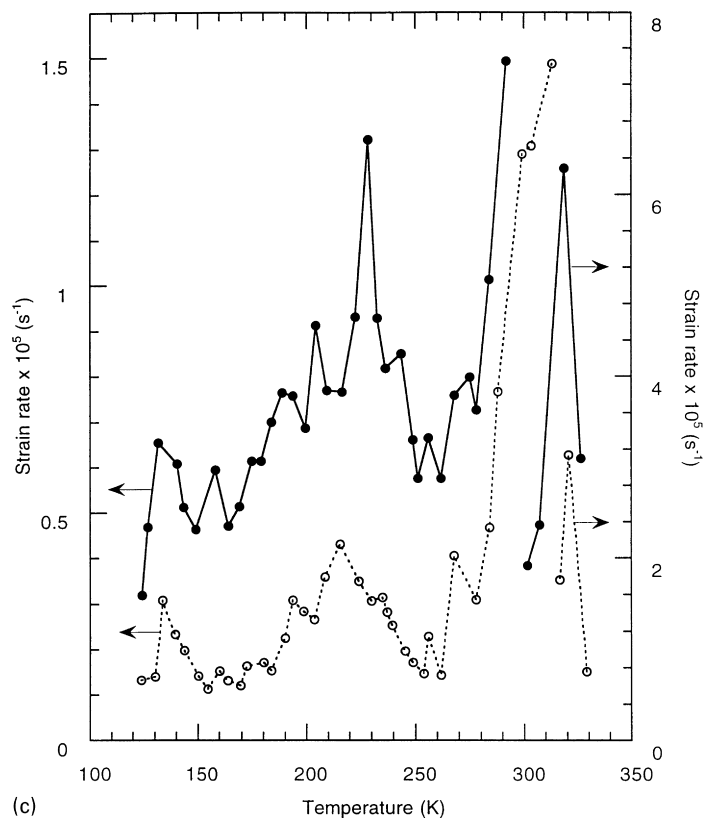
Fig. 5. (*continued*)

3. Results and discussion

3.1. Experimental parameter settings

As observed from the earlier studies, [15,18–21], the CRS, especially for complex systems, exhibit multiple creep rate $\dot{\varepsilon}$ peaks, irrespective of what the values of experimental parameters σ (applied stress) and t (time after loading) may be. An open question, however, deals with the choice of the values of σ which permit collection of the most representative CRS's. Optimization of this set of parameters, indeed, may depend on the mechanical characteristics of the samples, i.e. on the architectural characteristics of the networks (cross-link density and chain flexibility). In the case of the fully cross-linked network DGEBA–DDM at $t = 10$ s, the application of both $\sigma = 20$ and 40 MPa was examined. As shown in Fig. 4(a), the contour of the creep rate spectrum is much less broken at $\sigma = 20$ MPa than at $\sigma = 40$ MPa. In addition, it resembles much more, except in the low temperature range and near 300 K, to the loss modulus profile determined by dynamic mechanical analysis (DMA) (dotted line in the figure). Therefore, it seems to be convenient to set σ at 20 MPa, which is roughly the lowest value compatible with measurements of the creep rate with confidence. The undesirable distortions observed at $\sigma = 40$ MPa might be because of the increased effects of the mechanical activation of the sub-T_g relaxations and of

the inelastic deformation. As these conclusions hold for the different networks under study, the results discussed later refer systematically to the condition $\sigma = 20$ MPa. Let us now consider the influence of t, starting again with the case of DGEBA–DDM (Fig. 4(b)). As a general rule, the $\dot{\varepsilon}$ peak intensity drops with increasing t, because of the slowing down of the creep process with time for stresses which are much lower than the yield stress. One should notice, however, that this conclusion suffers from a few exceptions like for instance, at 270 K, the creep rate is the lowest for the shortest creep time (Fig. 4(b)). As explained in detail in a review article on the CRS technique [15], these peculiar effects have to do with the close neighboring of the measurement temperature to any transition temperature; they are associated with an unfortunate non-homogeneous step-like time evolution of the creep deformation. More interestingly, the best spectral resolution is achieved with this system at $t = 10$ s. As can be seen in the CRS's, the well defined peaks observed for $t = 10$ s at temperatures higher than 180 K degenerate at longer times (30 and 40 s) into a smooth plateau which is fairly distinguishable from a continuous baseline change. As long as the topological constraints diminish in the networks, the choice of the optimal value of t becomes less and less critical as the overall shape of the CRS does not change significantly as a function of time. These findings are illustrated in Fig. 5(a)–(c), relative to the rigid but loosely cross-linked network DGEBA–
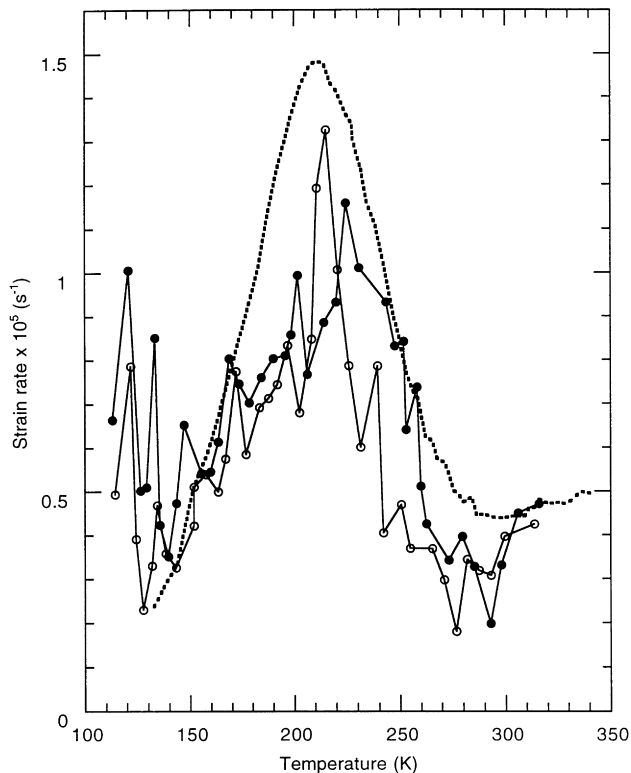
Fig. 6. CRS obtained at $\sigma = 20$ MPa and $t = 10$ s for two samples DGEBA–DDM/60BAN coming from two separate batches. The dotted line corresponds to the E'' dynamic mechanical spectrum at 1 Hz (data taken from Ref. [23]).

DDM/80BAN, to the aromatic and quasi-uncrosslinked system DGEBA-DDM/95BAN, and to the semi-aliphatic and quasi-uncrosslinked DGEBA–HMDA/95HA, respectively.

3.2. Principles for the analysis of the creep rate spectra

Owing to the high resolution of the spectra, it might be tempting to search for the individual meaning of each of the $\dot{\varepsilon}$ peaks. However, it should be borne in mind that peak multiplicity may be influenced by factors such as differences in local packing density, heterogeneities of cross-link density, fluctuations in the distance between the motional unit and the next cross-link, etc. In addition, it would be difficult to achieve the assignment of the multiple sub-T_g peaks in the CRS's only because of the mechanical data although complementary techniques and approaches could try to do so.

As a matter of fact, the reproducibility of the CRS's suffer from certain limitations. As shown in Fig. 6 relative to the DGEBA–DDM/60BAN network, incomplete coincidence in both amplitude ($\pm 30\% - 50\%$) and temperature location of the $\dot{\varepsilon}$ peaks was observed by the measurements performed on samples coming from different batches. This is probably the result of the cumulative effects of small differences in network architecture from one synthesis to
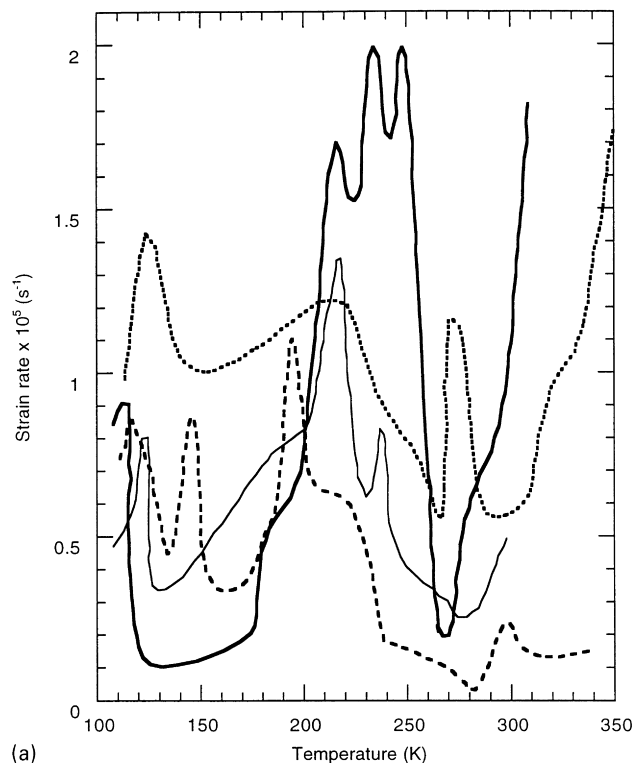
(a)
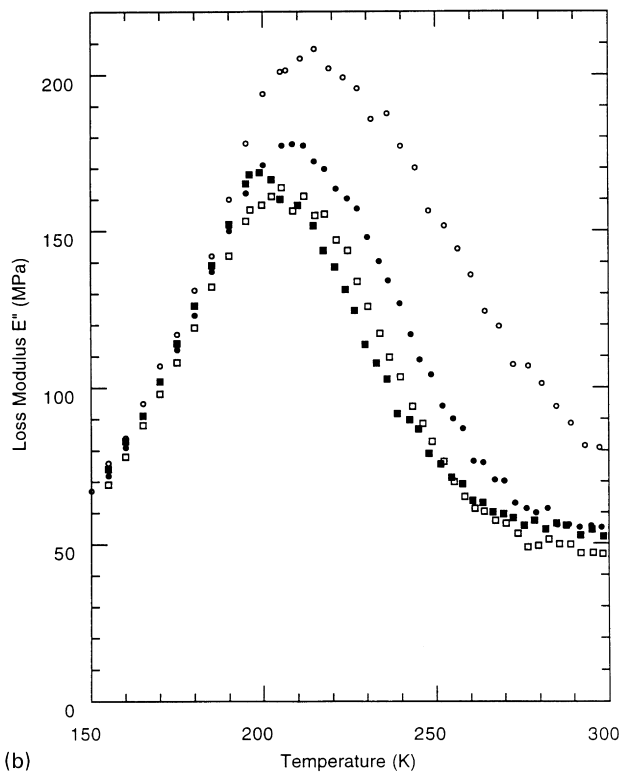
(b)

Fig. 7. Comparison of the sub-T_g responses in the DGEBA–DDM/BAN series (a) contours of the CRS at $\sigma = 20$ MPa and $t = 10$ s (——DGEBA–DDM; ——DGEBA–DDM/60BAN; - -DGEBA–DDM/80BAN; ··· DGEBA–DDM/95BAN). (b) E'' dynamic mechanical spectra at 1Hz (data taken from Ref. [23]) (open circles: DGEBA–DDM; filled circles: DGEBA–DDM/60BAN; open squares: DGEBA–DDM/80BAN; filled squares: DGEBA–DDM/95BAN).
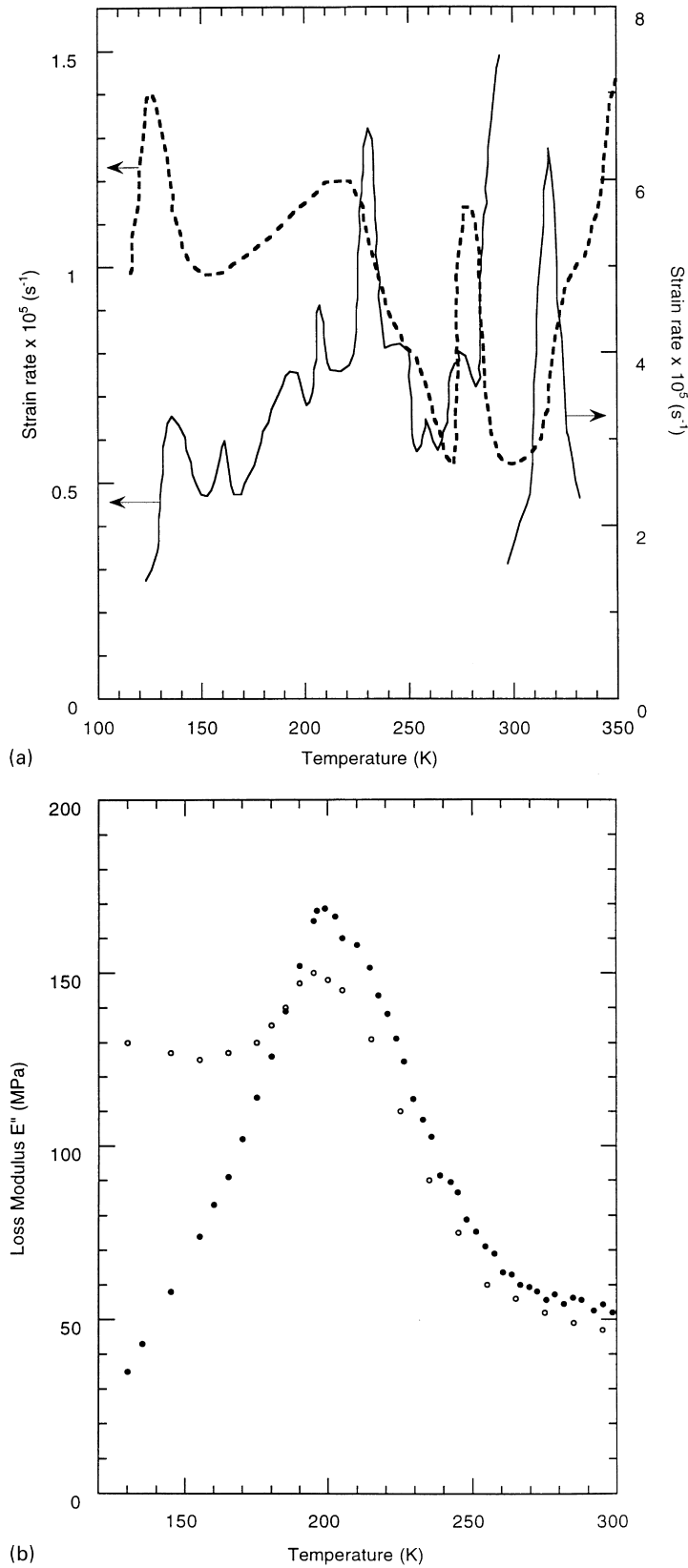
Fig. 8. Comparison of the sub-T_g responses of the quasi-uncross-linked systems. (a) contours of the CRS at $\sigma = 20$ MPa and $t = 10$ s (−−: DGEBA–DDM/95BAN; ——DGEBA–HMDA/95HA) (b) E'' dynamic mechanical spectra at 1 Hz (data taken from Ref. [23]) (filled circles: DGEBA–DDM/95BAN; open circles: DGEBA–HMDA/95HA).
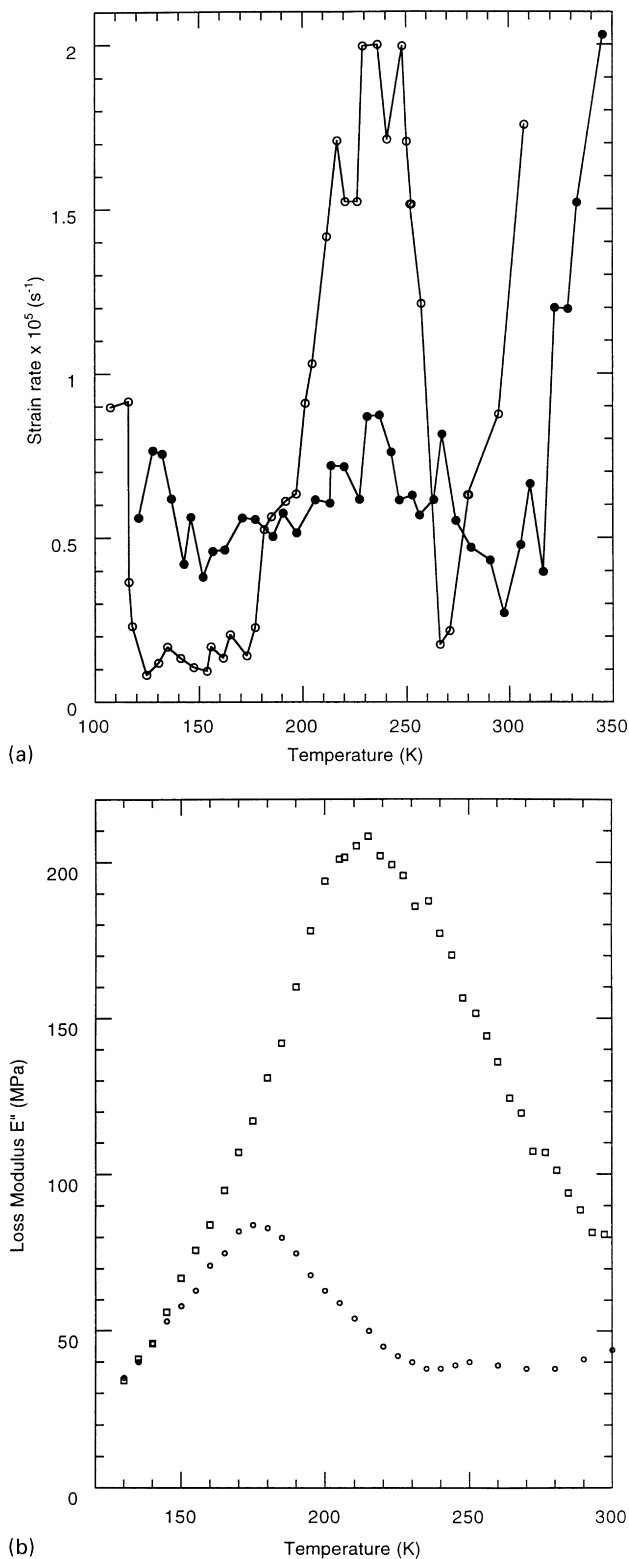
(a)

(b)

Fig. 9. Comparison of the sub-T_g responses of the pure DGEBA–DDM network and of the antiplasticized DGEBA–DDM/0.62AP network. (a) CRS at $\sigma = 20$ MPa and $t = 10$ s (open circles: neat network; filled circles: antiplasticized network) (b) E'' dynamic mechanical spectra at 1 Hz (data taken from Ref. [22]) (open squares: neat network; open circles: antiplasticized network).

the other and, eventually, of non-identity in the experimental conditions of CRS data collection. However, the relative heights of the major $\dot{\varepsilon}$ peaks in a given spectrum are preserved and characterize to some extent, the ability of the different types of motional units to relax in the sub-T_g region.

Moreover, as seen in Fig. 6, the rough envelope of the creep rate spectrum is quite stable in position along the temperature axis, irrespective of the sample under consideration. Except in the low temperature range, its smoothed shape highly resembles that of the loss modulus profile determined by DMA (dotted line in Fig. 6). This observation, which has been already mentioned earlier in the case of the network DGEBA–DDM (Fig. 4(a)), is verified, as a first approximation, for all the systems under study.

To go into a more quantitative analysis, comparison between creep rate and dynamic mechanical data should be made at the same frequency. In our conditions, creep is determined by the local shear strains and its rate decreases as long as the interferogram recording proceeds. In the case of creep rates determined at the time $t = 10$ s after loading, the experimental correlative frequency, ν_{CRS}, is given by the following equation;

$$\nu_{CRS} = 1/2\pi t \tag{3}$$

which is equal to 1.6×10^{-2} Hz. This means that the dynamic mechanical traces at $\nu_{DMA} = 1$ Hz should be shifted towards low temperatures to account for the difference in frequency. The temperature shift factors $\Delta T = (T_{DMA} - T_{CRS})$ can be evaluated by the well-known Arrhenius equation, knowing the activation energies, E_a, in different parts of the β-relaxation peak

$$\ln \nu_{CRS} - \ln \nu_{DMA} = \frac{E_a}{R}\left(\frac{1}{T_{DMA}} - \frac{1}{T_{CRS}}\right). \tag{4}$$

The value of the mean shift factor depends on the system considered as E_a and T_{DMA} are functions of the network architecture. Roughly speaking, the order of magnitude of ΔT is around 20°C, as calculated from the data relative to the maximum of the β-relaxation of DGEBA–DDM at 1 Hz [2]. Figs. 6–9 show a reasonable agreement between the positions of the maxima of the CRS contours and of the DMA traces on the temperature scale. Somewhat larger discrepancy is observed only for the network DGEBA–DDM (Fig. 4(a)). As a general rule, ΔT is comparable to the error bars on the $\dot{\varepsilon}$ peak location and therefore cannot be discussed in more details.

3.3. Relation between creep rate spectra and molecular mobility

The objective of this section is to analyze the CRS in relation with the chemical structure and molecular mobility of the network. To this end, the CRS's will be confronted with the literature available, and especially with the DMA data. As discussed earlier, we will focus here on the CRS's

Table 3
Characteristic temperatures of the CRS's at $\sigma = 20$ MPa and $t = 10$ s (The temperatures of the major events are underlined.)

System	Temperature (K)								
DGEBA–DDM	115			215	<u>230</u>	<u>245</u>		<u>~ 300</u>	
DGEBA–DDM/60BAN	120		185	<u>210</u>					
DGEBA–DDM/80BAN	120	145	<u>195</u>						
DGEBA–DDM/95BAN	<u>125</u>			215			270		350
DGEBA–HMDA/95HA	130		190	200	<u>230</u>		270	~ 300	315
DGEBA–DDM/0.62P	130				<u>230</u>		<u>270</u>	~ 310	

relative to the conditions $\sigma = 20$ MPa and $t = 10$ s. Even if our goal is restricted, as justified earlier, to the analysis of the main $\dot{\varepsilon}$ events, our choice was to illustrate in the article with the crude experimental data (Figs. 4–9), which exhibit many narrow peaks falling out of the scope of the discussion. In order to prevent any confusion for the reader, the characteristic temperatures of the $\dot{\varepsilon}$ peaks to be considered in the rest of the article are summarized in Table 3.

Firstly, let us compare the CRS's of the networks of the series DGEBA–DDM, which exhibit substantial differences in cross-link density (Table 2). For a simpler perception of the main $\dot{\varepsilon}$ peaks, the Fig. 7(a) shows the only contours of the spectra (without the data points). In the temperature range from 160 to about 280 K, the CRS's of the networks do not differ considerably by the number and the temperature location (with an accuracy of a few degrees) of the $\dot{\varepsilon}$ peaks. The main effect consists of redistribution of the amplitude of the spectral components. Significantly, a large increase in peak heights is observed for the network DGEBA–DDM, with much more distinct manifestation of the $\dot{\varepsilon}$ peaks at $\backsim$ 230 and 245 K. These trends are totally in accordance with the results of DMA, recalled in Fig. 7(b). Any increase in cross-link density leads to the increase of both the amplitude and the temperature range of the damping peak associated with the β relaxation. However, $\dot{\varepsilon}$ peaks are systematically observed irrespective of the cross-link density in the low-temperature range (120–150 K). In this case, the creep rates seem to be basically higher and the $\dot{\varepsilon}$ peaks more pronounced for the quasi-uncross-linked network. It is worth pointing out that in this temperature range, no marked mechanical losses has been reported in the DMA experiments. Therefore, in this particular situation, it would be possible to learn much more on molecular mobility from the CRS's than from the DMA traces.

In order to understand the molecular origin of this additional relaxation, which we propose to designate by γ', it is interesting to compare the behavior of the system DGEBA–DDM/95 BAN with that of the system DGEBA–HMDA/95HA. Both systems are quasi-uncross-linked materials (Table 2) which differ by the chemical nature (aromatic or aliphatic) of both cross-links and dangling units. At the first sight, the inspection of the high-temperature side of Fig. 8(a) reveals that the relevant CRS's are very much sensitive to the approach of the glass transition phenomenon where the maximum α relaxation, as determined from DMA

experiments at the frequency 1 Hz, was reported to occur at 329 K [6,23] and 359 K [23] for the systems DGEBA–HMDA/95HA and DGEBA–DDM/95BAN, respectively. This conclusion is rather expected and anyway goes beyond the scope of the present discussion. At a temperature of about 270 K, both materials exhibit a creep rate peak, which is probably screened by the cooperative β motions at higher cross-link density. Taking into account that this peak is present irrespective of the chemical nature of the amine hardener, it should result from motions of the DGEBA moieties. In the temperature range of about 160–260 K, the CRS's of both systems DGEBA–HMDA/95HA and DGEBA–DDM/95BAN are also sensitive to the β relaxation process, which is also observed in the DMA traces (Fig. 8(b)). Therefore, all the $\dot{\varepsilon}$ peaks over the range 160–270 K are supposed to be the reflect of both localized motions of the hydroxypropylether units and of ring flips of the bisphenol-A units [2,6,13]. Finally, the differences of the CRS's at very low temperatures is worth noting. The shape of the spectrum of DGEBA–HMDA/95HA can be justified by the occurrence of the γ relaxation of the amine methylene units [6], which is clearly apparent on the DMA trace also (Fig. 8b). The γ' peak around 120 K seems to be lacking in the CRS of DGEBA–HMDA/95HA. In addition, it is well known from NMR that the hydroxypropylether units [6] and the DGEBA aromatic rings [6,12] are strictly immobile at this very low temperature. Therefore, the γ' relaxation should result in the DDM/BAN series from DMA-inactive motions of the aromatic amine residues. One may tentatively suggest that the relevant motions would be the phenyl ring flips of the diphenylmethane units.

Finally, let us show that all the aforementioned conclusions are supported by the comparison of the behavior of the dense network DGEBA–DDM with that of its antiplasticized counterpart DGEBA–DDM/0.62AP. The CRS's are shown in Fig. 9(a). In the case of the antiplasticized material the huge increase in creep rate above 340 K is indicative of the gradual approach of the glass transition (the maximum α relaxation as determined from DMA experiments at 1 Hz, was 379 K [22]). In the intermediate temperature range (160–270 K), the drop in creep rate values as compared to the pure network is consistent with the DMA data (Fig. 9(b)), which were tentatively interpreted [2,6] as the disappearance of the cooperative motions of the

hydroxypropylether units. This behavior is also consistent with the NMR study of the "twin" system DGEBA–HMDA/0.62AP [9], which concluded that the antiplasticizer was able to hinder the motions of the CH_2 groups that are close to the nitrogen cross-links. The observation of a peak at 270 K on the spectrum of the antiplasticized network gives the further indication that the ring flips of the bisphenol-A units would not be concerned by the action of the antiplasticizer. This finding is in agreement with the location of the antiplasticizer in the networks as suggested by a recent REDOR NMR study [14]. Finally, the detection of significant creep rate peaks below 140 K in the antiplasticized material can be regarded as a confirmation of the assignment of the γ' relaxation to the phenyl ring flips of the amine residues, which are not supposed to be concerned by the action of the additive. The enhancement of the creep rate as compared with the pure network and the slight shift of the peak towards the higher temperatures may be justified by the fact that phenyl ring flips of the antiplasticizer molecules possibly occur in the same temperature range and may also affect the creep rate spectrum.

A complementary analysis of the cooperative character of the sub-T_g motions in these model epoxy networks will be the subject of a forthcoming publication.

References

[1] Gérard JF, Galy J, Pascault JP, Cukierman S, Halary JL. Polym Eng Sci 1991;31:615.

[2] Cukierman S, Halary JL, Monnerie L. Polym Eng Sci 1991;31:1476.

[3] Gallouedec F, Costa-Torro F, Lauprêtre F, Jasse B. J Appl Polym Sci 1993;47:823.

[4] Merritt ME, Heux L, Halary JL, Schaefer J. Macromolecules 1997;30:6760.

[5] Lauprêtre F, Eustache RP, Monnerie L. Polymer 1995;36:267.

[6] Heux L, Halary JL, Lauprêtre F, Monnerie L. Polymer 1997;38:1767.

[7] Yang L, Hristov HA, Yee AF, Gidley DW, Bauchière D, Halary JL, Monnerie L. Polymer 1995;36:3997.

[8] Rudnev SN, Oleinik EF. Vysokomol Soedin 1980;A22:2482.

[9] Heux L, Lauprêtre F, Halary JL, Monnerie L. Polymer 1998;39:1269.

[10] Dammont FR, Kwei TK. J Polym Sci A. 2 1967;5:761.

[11] Charlesworth JM. Polym Eng Sci 1988;28:230.

[12] Garroway AN, Ritchey MR, Moniz WB. Macromolecules 1982;15:1051.

[13] Shi JF, Inglefield PT, Jones AA, Meadows MD. Macromolecules 1996;29:605.

[14] Merrit ME, Goetz JM, Whitney D, Chang CP, Heux L, Halary JL, Schaefer J. Macromolecules 1998;31:1214.

[15] Peschanskaya NN, Yakushev PN, Sinani AB, Bershtein VA. Thermochim Acta 1994;238:429.

[16] Bershtein VA, Peschanskaya NN, Sinani AB, Stepanov VA. Fizika Tverdogo Tela (Sov Solid State Phys) 1980;22:767.

[17] Bershtein VA, Peschanskaya NN, Stepanov VA. Vysokomol Soedin 1980;A22:2246.

[18] Peschanskaya NN, Yakushev PN, Stepanov VA. Fizika Tverdogo Tela (Sov Solid State Phys) 1984;26:1202.

[19] Peschanskaya NN, Yakushev PN, Surovova VYu. Fizika Tverdogo Tela (Sov Solid State Phys) 1995;37:2602.

[20] Peschanskaya NN, Yakushev PN, Sinani AB, Bershtein VA. Macromol Symp 1997;119:79.

[21] Peschanskaya NN, Yakushev PN, Sinani AB, Bershtein VA. Third Intern Disc Meeting on Relaxations in Complex Systems, Vigo (Spain), 1997.

[22] Halary JL, Heux L, Rana D, Sauvant V, Monnerie L. Proc Amer Chem Soc PMSE Division 1996;75:358.

[23] Halary JL, Bauchière D, Lee PL, Monnerie L. Polimery 1997;42:86.